Reactive nanostructured membranes for water purification

Scott R. Lewis[a], Saurav Datta[a], Minghui Gui[a], Eric L. Coker[a], Frank E. Huggins[a,b], Sylvia Daunert[c], Leonidas Bachas[d], and Dibakar Bhattacharyya[a,1]

[a]Department of Chemical and Materials Engineering, University of Kentucky, Lexington, KY 40506-0046; [b]Consortium for Fossil Fuel Science, University of Kentucky, Lexington, KY 40506-0046; [c]Department of Biochemistry and Molecular Biology, University of Miami, Miami, FL 33136; and [d]Department of Chemistry, University of Miami, Miami, FL 33146

Edited by Benny D. Freeman, University of Texas at Austin, Austin, TX, and accepted by the Editorial Board April 19, 2011 (received for review January 24, 2011)

Many current treatments for the reclamation of contaminated water sources are chemical-intensive, energy-intensive, and/or require posttreatment due to unwanted by-product formation. We demonstrate that through the integration of nanostructured materials, enzymatic catalysis, and iron-catalyzed free radical reactions within pore-functionalized synthetic membrane platforms, we are able to conduct environmentally important oxidative reactions for toxic organic degradation and detoxification from water without the addition of expensive or harmful chemicals. In contrast to conventional, passive membrane technologies, our approach utilizes two independently controlled, nanostructured membranes in a stacked configuration for the generation of the necessary oxidants. These include biocatalytic and organic/inorganic (polymer/iron) nanocomposite membranes. The bioactive (top) membrane contains an electrostatically immobilized enzyme for the catalytic production of one of the main reactants, hydrogen peroxide (H_2O_2), from glucose. The bottom membrane contains either immobilized iron ions or ferrihydrite/iron oxide nanoparticles for the decomposition of hydrogen peroxide to form powerful free radical oxidants. By permeating (at low pressure) a solution containing a model organic contaminant, such as trichlorophenol, with glucose in oxygen-saturated water through the membrane stack, significant contaminant degradation was realized. To illustrate the effectiveness of this membrane platform in real-world applications, membrane-immobilized ferrihydrite/iron oxide nanoparticles were reacted with hydrogen peroxide to form free radicals for the degradation of a chlorinated organic contaminant in actual groundwater. Although we establish the development of these nanostructured materials for environmental applications, the practical and methodological advances demonstrated here permit the extension of their use to applications including disinfection and/or virus inactivation.

enzyme catalysis | functionalized membranes | pollutant | microfiltration | responsive materials

Providing access to safe drinking water has been identified as one, and possibly the most important, of the grand challenges facing scientists in the 21st century (1). The contamination of groundwater aquifers by toxic organic compounds is a widespread problem that prevents these potentially potable sources from being used for drinking water. In the United States, approximately two-thirds of the over 1,200 most serious hazardous waste sites in the nation are contaminated with trichloroethylene (TCE), a potentially carcinogenic compound. TCE and 2,4,6-trichlorophenol (TCP), a carcinogenic and persistent pollutant, represent the large class of chlorinated organics responsible for the contamination of many potential drinking water sources around the world.

Recent advances in membrane technology have led to an increased use of synthetic membranes for water treatment including the removal of viruses and unwanted chemicals from contaminated sources of water (2). Traditionally, synthetic membranes have been used as permeable barriers for the physical separation of two bulk phases, permitting the transport of solutes based on size or differences in diffusion/sorption rates. With the intent of imitating the multiple functionalities characteristic of naturally occurring membranes, various polymers, biological compounds, nanostructures, and functional groups have been incorporated onto the surfaces of synthetic membranes, extending their applicability to more advanced separation processes (3–9) and catalysis (10). By functionalizing these membranes with a stimuli-responsive polymer present as either grafted chains or a cross-linked network, the dimensions of the pores can be controlled by simple modulation of the stimulus (light, pH, ionic strength, etc.) resulting in the formation of a controllable nanoporous structure (11). When operated under pressure-driven convective flow, these membranes provide reactants rapid access to active sites, thereby minimizing the mass transfer limitations associated with other high surface area-to-volume materials. Nonetheless, these processes can be energy-intensive and the resulting concentrated waste stream must undergo further processing.

Various chemical-based treatment technologies also exist for the detoxification of contaminated water sources. Advanced oxidative reactions require the generation of free radicals, the highly reactive nature of which has been well-documented in medical literature (12), that can be utilized for the degradation of various pollutants (13) and disinfection (14). A well-known method of producing free radicals is via the reaction of either iron ions (Fe^{2+}/Fe^{3+}) or ferrihydrite/iron oxides with hydrogen peroxide (H_2O_2) (13, 15). The main reaction for the formation of free radicals from Fe^{2+} and H_2O_2 is as follows (15):

$$Fe^{2+} + H_2O_2 \rightarrow Fe^{3+} + OH^- + OH\bullet, \qquad [1]$$

where OH• is the hydroxyl radical. Although additional propagation reactions take place during this process (13) (*SI Text*), hydroxyl radicals are responsible for the majority of contaminant degradation, which proceeds as follows for a chlorinated organic compound, A (16):

$$A + OH\bullet \longrightarrow I \xrightarrow{OH\bullet} P + Cl^-, \qquad [2]$$

where I represents the intermediate compounds formed and P represents the oxidized products of the chlorinated organics. Although these free radical reactions are highly effective for

Author contributions: S.R.L., S. Datta, and D.B. designed research; S.R.L., S. Datta, M.G., and E.L.C. performed research; F.E.H. contributed new reagents/analytical tools; S. Daunert and L.B. were involved in the bioactive part of the work; S.R.L., S. Datta, and D.B. analyzed data; and S.R.L., S. Datta, S. Daunert, L.B., and D.B. wrote the paper.

The authors declare no conflict of interest.

This article is a PNAS Direct Submission. B.D.F. is a guest editor invited by the Editorial Board.

[1]To whom correspondence should be addressed at: Department of Chemical and Materials Engineering, University of Kentucky, Lexington, KY 40506-0046. E-mail: db@engr.uky.edu.

This article contains supporting information online at www.pnas.org/lookup/suppl/doi:10.1073/pnas.1101144108/-/DCSupplemental.

ENVIRONMENTAL SCIENCES

degrading organic contaminants, they may require the addition of expensive reagents and downstream processing. However, by integrating the oxidative reactions into a membrane-based process through the use of uniquely functionalized membranes in sequential configuration (17), we are able to minimize the disadvantages associated with the individual processes.

Herein, we synthesized reactive nanostructured stacked membrane systems with tunable pore size in order to conduct environmentally important toxic organic oxidative degradation reactions by using glucose as the source of H_2O_2 (Fig. 1*A*). By synthesizing H_2O_2 in the pores of the top membrane, we are able to regulate its generation, thus eliminating unnecessary waste. In order to achieve this, the pores of the top membrane were functionalized using a versatile polycation/polyanion layer-by-layer (LbL) assembly technique (18–21) for the immobilization of negatively charged glucose oxidase (GOx), which converts glucose and oxygen to H_2O_2 and gluconic acid (22) (Fig. 1*B*). These products are convectively transported to the bottom membrane where H_2O_2 reacts with the bound iron species (iron ions or ferrihydrite/iron oxide nanoparticles) contained within a poly (acrylic acid) (PAA) network, forming the free radicals necessary for contaminant degradation (Fig. 1*D*). This PAA network is a pH-responsive gel, providing the opportunity for controlled opening and closing of the membrane pores (Fig. 1 *C* and *D*). Furthermore, to extend this work to real-world applications, we used groundwater from a contaminated aquifer to demonstrate how ferrihydrite/iron oxide nanoparticles synthesized within these PAA-functionalized membranes are capable of oxidizing toxic organics in the presence of H_2O_2.

Results and Discussion

Functionalizing the pores of a support membrane with PAA creates a nanostructured material ideal for iron ion immobilization (for reaction with H_2O_2) due to its high ion exchange capacity (23) and the stability of immobilized iron ions in the presence of other cations (*SI Text*). To synthesize this membrane, a network of PAA was created within the pores of a poly(vinylidene fluoride) (PVDF) membrane using a simple in situ polymerization technique. Given the variability associated with this process, it is important to ascertain the uniformity of the PAA coating within the PVDF membrane. A cationic fluorescent dye, thionine, was bound to the carboxylate groups of PAA via ion exchange for subsequent analysis with confocal laser scanning microscopy (CLSM). Through the use of CLSM, we are able to observe thionine binding through the depth of the membrane while in a hydrated state and without altering the membrane structure. The CLSM images in Fig. 2*A* constitute the average fluorescence of multiple images taken at different depths throughout the PVDF-PAA and unmodified PVDF membranes (*SI Text*). The fluorescence of the blank PVDF membrane was much lower in intensity than the PVDF-PAA membrane and was due to the background fluorescence of the membrane itself and/or physically adsorbed thionine, indicating the presence of PAA throughout the PVDF-PAA membrane pores. SEM images of the cross-section (no thionine) of the dried membrane (Fig. 2*B*) provided visual evidence of the PAA coating. The presence of PAA in the membrane pores was further verified through the detection of oxygen via energy dispersive X-ray (EDX) analysis (Fig. S1).

The pH-responsive behavior of the PAA network ($pK_a \sim 4.7$) permits controlled opening and closing of the PAA-coated membrane pores (24). This can be used to bring immobilized reactants into closer proximity to the feed solution permeating through the membrane, vary the residence time, or remove entrapped precipitates from the membrane pores (by collapsing the PAA domain at lower pH). In addition to tuning pore size via pH alterations, divalent cation (Fe^{2+} and Ca^{2+}) capture for the modulation of water flux through the membrane was investigated. Fig. 3 shows the cumulative quantities of Ca^{2+} and Fe^{2+} captured in the membrane during operation under convective flow as well as the effect this had on the water flux through the membrane. Within the first 5 min, a slight drop in pH was observed, accounting for the initial increase in flux. However, once the pH of the permeate had stabilized at approximately 4.4, the flux continued to increase with time. Because of the increased shielding of the negatively charged carboxylate groups by divalent cations in comparison to the displaced monovalent cations (Na^+ and H^+) (25), their capture resulted in increased water flux through the membrane, indicating a collapse of the PAA gel.

By immobilizing iron ions in the PVDF-PAA domain, the iron-functionalized membrane provides the platform needed for the generation of free radicals from H_2O_2. Previous work has shown the generation of free radicals within PVDF-PAA-Fe^{3+} membrane pores to be effective for the degradation of pentachlorophenol in water (23). In order to ensure that Fe^{2+} was being captured by the PAA network and not precipitating in the membrane pores, it was necessary to monitor the release of the cation displaced by Fe^{2+} during ion exchange. For this reason, and to prevent pH drop during Fe^{2+} capture, the PVDF-PAA

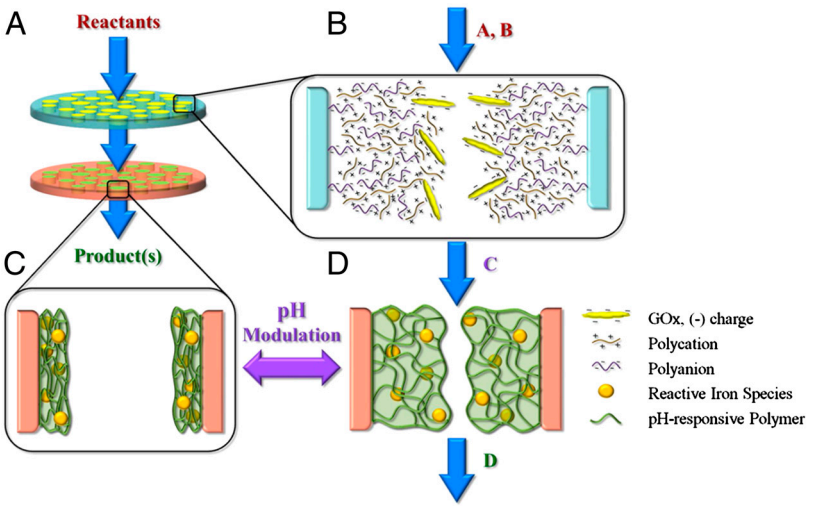

Fig. 1. Schematic of reactive nanostructured stacked membrane system. (*A*) Setup of stacked membrane system consisting of two membranes of different functionality operated via convective flow. (*B*) Pore of top membrane with layer-by-layer polycation/polyanion assembly containing electrostatically immobilized GOx for the conversion of reactants A + B → C. (*C*) Pore of bottom membrane consisting of pH-responsive PAA gel with immobilized iron species in collapsed state. (*D*) Pore of bottom membrane after exposure to increased pH causing gel to swell; reactive iron species catalyzes conversion of C → D.

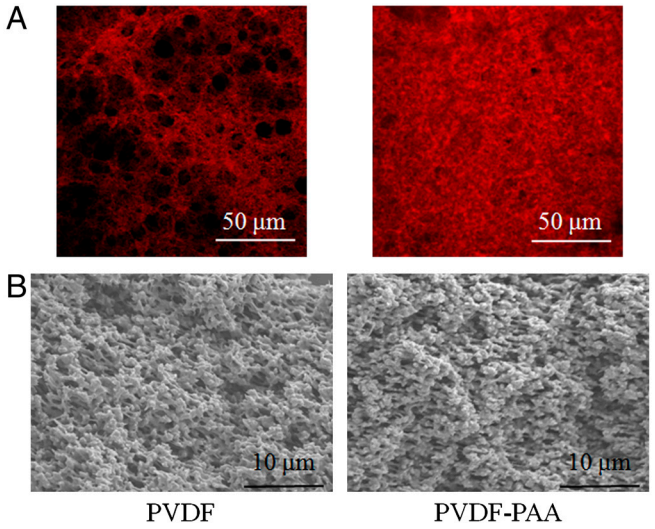

Fig. 2. CLSM and SEM imaging of PAA gel coverage of PVDF membrane. (*A*) CLSM fluorescent images of PVDF and PVDF-PAA membranes stained with thionine (488-nm excitation). Brighter areas indicate higher concentrations of thionine. (*B*) SEM images of PVDF and PVDF-PAA membrane cross-sections.

membranes were preloaded with Na^+ (PVDF-PAA-Na^+). It was observed that for every mole of Fe^{2+} captured, approximately 2 mol of Na^+ were released, indicating successful capture in the PAA domain. During loading, Fe^{2+} was immobilized through the entire thickness of the membrane, as confirmed by EDX (Fig. S1). It is important to note that there was no evidence of iron precipitation during loading and no leaching of iron from the membrane was detected during experimentation. Although immobilized Fe^{2+} was shown to be less stable than Fe^{3+} in the presence of Ca^{2+} (*SI Text*), its increased rate of OH• production from H_2O_2 in comparison to Fe^{3+} in the solution phase could make it more suitable for contaminant degradation in the membrane domain.

Although the possibility exists to reduce Fe^{3+} to Fe^{2+} via addition of a reducing agent, the unloading and reloading of iron can be easily achieved due in part to the pH responsiveness of the gel. To demonstrate the ease with which the iron ions can be unloaded from these membranes, two membranes, one containing Fe^{2+} and the other containing Fe^{3+}, were added to separate solutions under acidic conditions, resulting in the release of the iron ions from both membranes. Fe^{2+} was subsequently recaptured within the PAA gel with no detectable loss of ion exchange capacity (see Table S1).

The PVDF-PAA membrane is valuable not only for the immobilization of iron ions, but also, through the addition of a layer of positively charged poly(allylamine hydrochloride) (PAH), for the immobilization of negatively charged GOx (pI = 4.2) at near-neutral pH (26) (PVDF-PAA-PAH-GOx) (Fig. 4). Previous

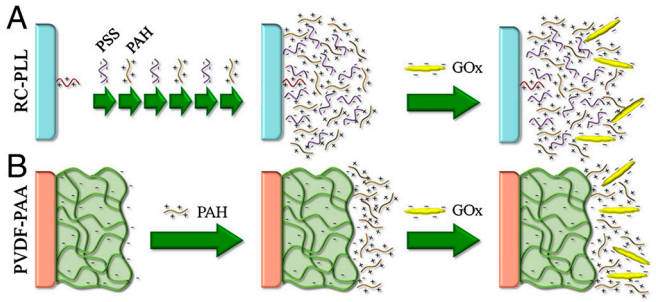

Fig. 4. Schematic of GOx immobilization in multiple membrane platforms. (*A*) RC-LbL-GOx: RC-PLL membrane with LbL assembly of alternating layer of PSS and PAH and subsequent GOx immobilization. (*B*) PVDF-PAA-PAH-GOx: PVDF-PAA membrane with an electrostatically immobilized layer of PAH and subsequent GOx immobilization.

work has shown that immobilization of enzymes via electrostatic interaction provides stability comparable to covalent attachment, yet maintains high activity more characteristic of the enzyme in solution (26). Although this PVDF-based system is suitable for the generation of H_2O_2, here, we demonstrate how another readily available supporting material, regenerated cellulose (RC), can be functionalized and used for the same purpose (Fig. 4). A net positively charged LbL assembly was created within the RC membrane pores through the covalent attachment of a layer of poly(L-lysine-hydrochloride) (PLL) to the epoxide-activated RC followed by the addition of alternating layers of poly(styrene sulfonate) (PSS) and PAH (RC-PLL-$(PSS\text{-}PAH)_3$ or RC-LbL) by electrostatic interaction, providing an ideal platform for the immobilization of negatively charged GOx (RC-LbL-GOx) (Fig. 4 and *SI Text*). The activity of the immobilized GOx, as measured by H_2O_2 production under convective flow, was constant at a fixed residence time (flow rate) (Fig. S2). By varying the concentration of glucose in the feed, the quantity of H_2O_2 produced can be easily manipulated, as indicated by the steady-state concentrations of H_2O_2 in the permeate. No leakage of GOx was detected during these experiments, demonstrating the stability of the immobilized GOx inside the RC-LbL membrane. After multiple uses, the GOx lost a small amount of activity; however, the LbL assembly allows for the reintroduction of fresh GOx to compensate for this loss in activity.

To demonstrate the effectiveness of the nanostructured stacked-membrane system, the oxidative degradation of TCP was carried out with a configuration consisting of the RC-LbL-GOx membrane on top of the PVDF-PAA-Fe^{2+} membrane (Fig. 5*A*). The process began by convectively permeating an oxygen-saturated solution of TCP and glucose through the top membrane where GOx converts glucose and oxygen to H_2O_2 and gluconic acid, leaving TCP unaffected. Upon entering the bottom membrane, H_2O_2 reacts with the immobilized Fe^{2+} (reaction **1**), generating hydroxyl radicals that react with TCP (reaction **2**). Although it is feasible to create a single membrane with both GOx and Fe^{2+} immobilized, it was necessary to use two separate

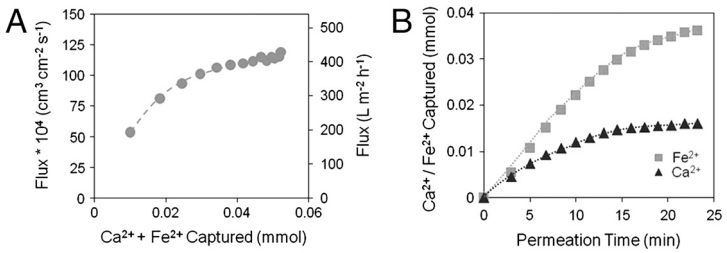

Fig. 3. Divalent cation-responsive water flux through PVDF-PAA membrane. (*A*) Water flux as a function of cumulative divalent cation (Fe^{2+} and Ca^{2+}) loading. (*B*) Cumulative divalent cation capture with time. Feed contains 0.50 mmol/L Fe^{2+} and 0.50 mmol/L Ca^{2+}; permeated at 1.4 bar; feed pH 5.0; permeate pH 4.4; external membrane area = 13.2 cm^2; (mol $Na^+ + H^+$ released)/(mol $Fe^{2+} + Ca^{2+}$ captured) = 2.1 ± 0.5.

membranes so as to avoid the deactivation of the enzyme by free radicals. Maintaining positive pressure drop across the membrane stack prevents free radicals from entering the top membrane.

Using a constant residence time, the initial conversion of TCP was 100%, but decreased with time, reaching 55–70% after 30 min (Fig. 5*B*). This decrease in TCP conversion is characteristic of these PVDF-PAA-Fe^{2+} membranes as the immobilized Fe^{2+} is converted to Fe^{3+}, reducing the rate of H_2O_2 decomposition and hence free radical production (Fig. S3 and *SI Text*). Note that each time point in Fig. 5*B* represents the steady-state conversion of TCP for the particular ratio of Fe^{2+}:Fe^{3+} that is present in the membrane at that time. As the free radical degradation of TCP progresses, various intermediates are formed and the attached chlorine atoms are released from the molecule as chloride ions. Chloride formation and TCP concentration in the permeate were monitored to ensure degradation via oxidation (Fig. 5*B*). Although the TCP conversion initially decreased, the ratio of mole Cl^- formed to mole TCP reacted remained relatively constant (approximately 2) through the entire experiment, indicating significant TCP degradation (maximum Cl^- released per TCP molecule is 3). The TCP conversion can be easily adjusted by varying the amount of iron loading, the rate of H_2O_2 production, the pore size via change in stimulus, the thickness of the membranes used, and/or residence time through pressure modulation. It should be noted that these residence times are calculated for the entire membrane, not individual pores (*SI Text*).

Although the bottom membrane in this stacked configuration contains iron ions, various forms of ferrihydrite/iron oxide nanoparticles can be synthesized in the membrane domain for similar oxidative reactions. These nanoparticles provide greater reaction rates than their bulk counterparts (27), and with the addition of H_2O_2, many of these oxides are capable of catalyzing the oxidative degradation of organic compounds (28). Furthermore, by using membranes impregnated with these inexpensive catalysts, additional separations for nanoparticle removal can be avoided. Our previous work has demonstrated the effective reductive dechlorination of contaminants via the use of zero-valent iron and bimetallic nanoparticles immobilized in the membrane domain (29). However, a wider range of contaminants can be detoxified by using the oxidants formed from the reaction of a different iron-based nanoparticle, ferrihydrite/iron oxide, and H_2O_2. Additionally, the efficiency with which these materials utilize H_2O_2 (i.e., mole contaminant degraded per mole H_2O_2 consumed) depends on the structure and surface chemistry of the iron oxides (28). At near-neutral pH, this efficiency could be higher for the iron oxide nanoparticles than similar materials used for H_2O_2 decomposition, thereby making their use advantageous.

Whereas other methods use elevated temperatures for ferrihydrite/iron oxide synthesis within a porous, ion exchange membrane structure functionalized via photografting (30), here, we synthesize ferrihydrite/iron oxide nanoparticles within an easily fabricated PVDF-PAA membrane at room temperature using one of two methods. The first entails direct precipitation of the iron species within the membrane pores; the second requires the synthesis of zero-valent iron nanoparticles within the membrane pores, which then undergo deliberate oxidation to form Fe/Fe_xO_y core/shell nanoparticles. Analysis of the membranes via Mössbauer spectrometry confirmed the presence of ferrihydrite/iron oxide (Fig. 6*A*) for both methods (*SI Text*). The average nanoparticle diameter for the first and second synthesis methods were determined by SEM to be 37 ± 14 nm (Fig. 6*B*) and 53 ± 17 nm (base nanoparticle diameter) (Fig. 6*C*), respectively. The PVDF-PAA membrane serves to limit nanoparticle aggregation, prevent nanoparticle loss, and permit the recapture of the iron ions as the nanoparticles dissolve, providing an opportunity to resynthesize the nanoparticles in the membrane domain.

In order to demonstrate the applicability of this technology to the remediation of contaminated water, PVDF-PAA membranes with immobilized Fe/Fe_xO_y nanoparticles (8.7 ± 0.4 mg Fe as Fe/Fe_xO_y) and H_2O_2 (40 mmol/L) were added to groundwater collected from the areas surrounding the US Department of Energy Paducah Gaseous Diffusion Plant Superfund Site. H_2O_2 was added to the solution in the reaction vessel containing the PVDF-PAA membranes with immobilized Fe/Fe_xO_y nanoparticles and 0.28 mmol/L TCE to initiate the reaction. The degradation of TCE due to the membrane-immobilized Fe/Fe_xO_y nanoparticles was 71 ± 3% in the groundwater sample compared to 80 ± 11% in deionized water after 33 h. This degradation was confirmed by the generation of approximately 3 mol chloride/mol TCE degraded, indicating successful removal of TCE even in the presence of natural groundwater constituents. This long reaction time represents the worst-case scenario of the composite membrane reactivity because they were used in a batch reaction and therefore relied on diffusion to transport the reactants to the immobilized nanoparticles. Operating these membranes under

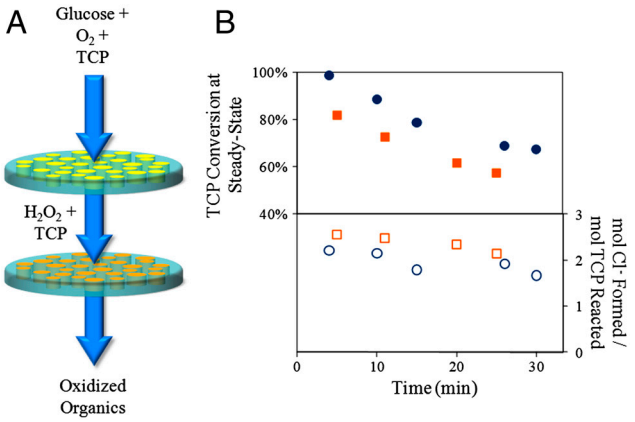

Fig. 5. Model compound degradation from water in a reactive nanostructured stacked membrane system. (*A*) Schematic of stacked membrane system for degradation of TCP using glucose and oxygen. Top membrane contains GOx electrostatically immobilized in LbL assembly; bottom membrane contains Fe^{2+} immobilized in a PVDF-PAA membrane. (*B*) TCP conversion at steady-state and Cl^- formation as a function of time. Squares: 0.14 mmol/L TCP in feed; circles: 0.07 mmol/L TCP in feed. Maximum mol Cl^- formed/mol TCP reacted = 3. Steady-state concentration of H_2O_2 from the first membrane is 0.1 mmol/L (circles) and 0.13 mmol/L (squares), Fe loading = 0.09 mmol, pH 5.5, residence time in the top membrane = 2.7 s, residence time in the bottom membrane = 2 s.

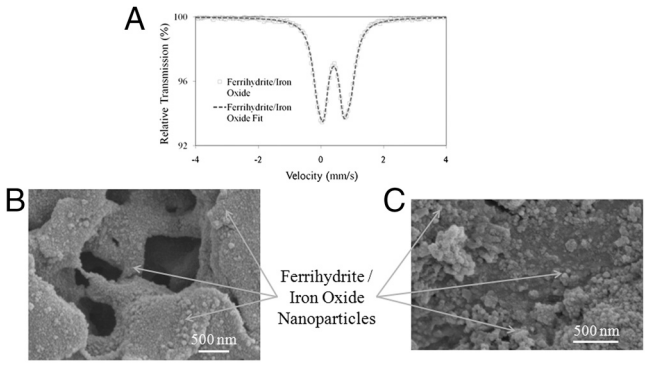

Fig. 6. Ferrihydrite/iron oxide nanoparticles synthesized in PVDF-PAA membrane pores. (*A*) Mössbauer spectra of membrane-immobilized ferrihydrite/iron oxide nanoparticles. (*B*) SEM of immobilized ferrihydrite/iron oxide nanoparticles synthesized via direct precipitation. (*C*) SEM of immobilized ferrihydrite/iron oxide nanoparticles synthesized via zero-valent iron oxidation.

diffusion-limited conditions would be beneficial for applications including permeable reactive barriers where extensive reaction times are common. Based on the batch reaction kinetics, operation under convective flow would require a residence time of 14 min to achieve approximately 71% TCE conversion in the groundwater compared to the 33 h for the batch reaction.

One advantage of these systems over PVDF-PAA-Fe^{2+} is that the immobilized nanoparticles will not be displaced by divalent cations permeating through the membrane. As expected, the immobilization of the Fe/Fe_xO_y nanoparticles decreased water flux through the PVDF-PAA membranes (Fig. S4). However, as demonstrated in Fig. 3*A*, one would expect the presence of multivalent ions in the groundwater feed (pH 7.5 with 0.6 mmol/L Ca^{2+}) to lead to an increase in water flux when compared to that of deionized water (pH 5.5). Indeed, this was the case and is an important demonstration of how the responsive behavior of the PVDF-PAA membrane can be utilized to increase the water flux through the membrane even at near-neutral pH with immobilized iron oxide nanoparticles.

We have demonstrated that through the utilization of this reactive, nanostructured, two-membrane stacked system, harmful organic contaminants can be degraded through the addition of a substrate, glucose, which is enzymatically converted to H_2O_2, thereby eliminating the need for additional chemical reagents. Additionally, we have shown how a common PVDF-PAA membrane provides an excellent platform for iron ion capture, enzyme immobilization, and ferrihydrite/iron oxide nanoparticle synthesis. The immobilized ferrihydrite/iron oxide nanoparticles proved to be effective for the degradation of a toxic organic contaminant in actual groundwater. The effectiveness of these reactive, nanostructured multimembrane systems presents an opportunity for conducting other complex reaction sequences quickly and efficiently.

Materials and Methods

Materials. Hydrophobic PVDF membranes (450-nm pore diameter, thickness of 125 μm, 75% porosity, as supplied by the manufacturer) and hydrophilic PVDF membranes (650-nm pore diameter, 125 μm thickness, 70% porosity, as supplied by the manufacturer) were purchased from Millipore Corporation. RC membranes were obtained from Sartorius Inc. The enzyme glucose oxidase from *Aspergillus niger* (GOx, Product No. G0543, MW 160000), β-D(+)-glucose (MW 180), and PLL (MW 105500, with repeat unit MW of 164.5) were purchased from Sigma. PSS (MW 70000, with repeat unit MW of 206), PAH (MW 56000, with repeat unit MW of 93.5), benzoyl peroxide, trimethylolpropane triacrylate (TMPTA), anhydrous toluene, and acrylic acid were purchased from Sigma-Aldrich. The reagents for Bradford assay were purchased from Bio-Rad Laboratories. Unless otherwise noted, the remaining chemicals, were purchased from Fisher Scientific.

RC-LbL-GOx Assembly. LBL assembly in RC membranes (200-nm pore diameter, 125 μm thickness): Epoxide groups were attached in RC membrane by permeating 100 mL of 5% solution of epichlorohydrin in 0.5 M NaOH at 50 °C. Then, the epoxide-activated RC membrane was reacted (covalent bonding) with the terminal amine group of PLL by permeating 100 mL of 40-ppm aqueous solution of PLL (4 mg or 0.039 μmol PLL) at 0.07 bar (1 psi) pressure and a pH of 9.3. The subsequent layer formation steps were carried out electrostatically at a working pH of 6 and in the presence of 0.25 M NaCl. The second layer of PSS was attached by permeating 100 mL of a 400-ppm solution of PSS (40 mg PSS, 0.2 mmol of negative charges) at pH 6. The next layer of PAH was formed by permeating 100 mL of a 300-ppm solution of PAH (30 mg PAH, 0.3 mmol of positive charges) at pH 6. After this, two more bilayers of PSS-PAH were attached in the membrane to obtain a net positively charged RC-PLL-$(PSS\text{-}PAH)_3$ membrane. GOx was immobilized electrostatically in this membrane by permeating 100 mL of a 25-ppm solution at pH 6. The GOx immobilized membranes were stored at 4 °C. A reaction mixture containing either 0.15 or 1 mmol/L glucose was prepared in O_2-saturated 50 mmol/L sodium acetate–acetic acid buffer of pH 5.5 and permeated through a RC-LbL-GOx membrane under N_2 atmosphere. Permeates were collected and analyzed for H_2O_2.

PVDF-PAA-Fe^{2+} Membrane Synthesis. A method reported by Gabriel and Gillberg (31) was followed to functionalize the pores of hydrophobic PVDF membrane (450-nm pore diameter, 125-μm thickness) with PAA (PVDF-PAA) by in situ polymerization of acrylic acid. The polymerization solution contained 70 wt % toluene, 30 wt % acrylic acid, 0.5 wt % benzoyl peroxide (initiator), and 1.2 wt % TMPTA (cross-linker) by weight. After polymerization, PAA was converted to Na form by permeating 0.1 M NaOH through the PVDF-PAA membrane. Then, 100 mL of a 3.8 mmol/L solution of $FeCl_2{\cdot}4H_2O$ in deoxygenated water (pH of 5–5.5) was permeated to immobilize Fe^{2+}. Prior to and after the ion exchange step, the membrane matrix was washed with copious amount of deoxygenated water. Because Fe^{2+} is prone to oxidation by O_2, these membranes were used immediately.

Reactive Nanostructured Stacked Membrane System for TCP Degradation. The composite membrane reactor was formed by stacking the RC-LbL-GOx membrane on top of the Fe^{2+} immobilized PVDF membrane in a convective flow cell. A reaction mixture containing either 0.07 or 0.14 mmol/L TCP and 1 mmol/L β-D(+)-glucose, simply referred to as glucose in the text, was prepared in O_2-saturated sodium acetate-acetic acid buffer of pH 5.5, and permeated through the stacked membrane system under N_2 atmosphere.

For details on other materials and methods, please see *SI Text*.

ACKNOWLEDGMENTS. The authors thank Joseph Amundson for experimental contributions and Mr. John May for analytical assistance. This work was funded by National Institute of Environmental Health Sciences-Superfund Research Program (Grant P42ES007380), Department of Energy-Kentucky Research Consortium for Energy and Environment, and National Science Foundation-Integrative Graduate Education and Research Traineeship programs. E.C. was funded by the NSF/REU program.

1. Omenn GS (2006) Grand challenges and great opportunities in science, technology, and public policy. *Science* 314:1696–1704.
2. Shannon MA, et al. (2008) Science and technology for water purification in the coming decades. *Nature* 452:301–310.
3. Kumar A, Srivastava A, Galaev IY, Mattiasson B (2007) Smart polymers: Physical forms and bioengineering applications. *Prog Polym Sci* 32:1205–1237.
4. Stuart MAC, et al. (2010) Emerging applications of stimuli-responsive polymer materials. *Nat Mater* 9:101–113.
5. Jirage KB, Hulteen JC, Martin CR (1997) Nanotubule-based molecular-filtration membranes. *Science* 278:655–658.
6. Lee SB, et al. (2002) Antibody-based bio-nanotube membranes for enantiomeric drug separations. *Science* 296:2198–2200.
7. Letant SE, Hart BR, Van Buuren AW, Terminello LJ (2003) Functionalized silicon membranes for selective bio-organism capture. *Nat Mater* 2:391–396.
8. Merkel TC, et al. (2002) Ultrapermeable, reverse-selective nanocomposite membranes. *Science* 296:519–522.
9. Park HB, et al. (2007) Polymers with cavities tuned for fast selective transport of small molecules and ions. *Science* 318:254–258.
10. Lu Y, Mei Y, Drechsler M, Ballauff M (2006) Thermosensitive core-shell particles as carriers for Ag nanoparticles: Modulating the catalytic activity by a phase transition in networks. *Angew Chem Int Ed Engl* 45:813–816.
11. Wandera D, Wickramasinghe SR, Husson SM (2010) Stimuli-responsive membranes. *J Membr Sci* 357:6–35.
12. Beckman JS, Beckman TW, Chen J, Marshall PA, Freeman BA (1990) Apparent hydroxyl radical production by peroxynitrite—Implications for endothelial injury from nitric-oxide and superoxide. *Proc Natl Acad Sci USA* 87:1620–1624.
13. Pignatello JJ, Oliveros E, MacKay A (2006) Advanced oxidation processes for organic contaminant destruction based on the Fenton reaction and related chemistry. *Crit Rev Env Sci Technol* 36:1–84.
14. Kohanski MA, Dwyer DJ, Collins JJ (2010) How antibiotics kill bacteria: From targets to networks. *Nat Rev Microbiol* 8:423–435.
15. Barb WG, Baxendale JH, George P, Hargrave KR (1949) Reactions of ferrous and ferric ions with hydrogen peroxide. *Nature* 163:692–694.
16. Benitez FJ, Beltran-Heredia J, Acero JL, Rubio FJ (1999) Chemical decomposition of 2,4,6-trichlorophenol by ozone, Fenton's reagent, and UV radiation. *Ind Eng Chem Res* 38:1341–1349.
17. Matson SL, Quinn JA (1986) Membrane reactors in bioprocessing. *Ann NY Acad Sci* 469:152–165.
18. Bruening ML, Dotzauer DM, Jain P, Ouyang L, Baker GL (2008) Creation of functional membranes using polyelectrolyte multilayers and polymer brushes. *Langmuir* 24:7663–7673.
19. Caruso F, Lichtenfeld H, Giersig M, Mohwald H (1998) Electrostatic self-assembly of silica nanoparticle—Polyelectrolyte multilayers on polystyrene latex particles. *J Am Chem Soc* 120:8523–8524.
20. Decher G (1997) Fuzzy nanoassemblies: Toward layered polymeric multicomposites. *Science* 277:1232–1237.
21. Tang ZY, Wang Y, Podsiadlo P, Kotov NA (2006) Biomedical applications of layer-by-layer assembly: From biomimetics to tissue engineering. *Adv Mater* 18:3203–3224.

22. Duke FR, Weibel M, Page DS, Bulgrin VG, Luthy J (1969) Glucose oxidase mechanism. Enzyme activation by substrate. *J Am Chem Soc* 91:3904–3909.
23. Lewis S, Smuleac V, Montague A, Bachas L, Bhattacharyya D (2009) Iron-functionalized membranes for nanoparticle synthesis and reactions. *Sep Sci Technol* 44:3289–3311.
24. Hu K, Dickson JM (2009) In vitro investigation of potential application of pH-sensitive poly(vinylidene fluoride)-poly(acrylic acid) pore-filled membranes for controlled drug release in ruminant animals. *J Membr Sci* 337:9–16.
25. Karppi J, Akerman S, Akerman K, Sundell A, Penttila I (2010) Adsorption of metal cations from aqueous solutions onto the pH responsive poly(vinylidene fluoride grafted poly(acrylic acid) (PVDF-PAA) membrane. *J Polym Res* 17:71–76.
26. Datta S, Cecil C, Bhattacharyya D (2008) Functionalized membranes by layer-by-layer assembly of polyelectrolytes and in situ polymerization of acrylic acid for applications in enzymatic catalysis. *Ind Eng Chem Res* 47:4586–4597.
27. Hermanek M, Zboril R, Medrik N, Pechousek J, Gregor C (2007) Catalytic efficiency of iron(III) oxides in decomposition of hydrogen peroxide: Competition between the surface area and crystallinity of nanoparticles. *J Am Chem Soc* 129:10929–10936.
28. Huang HH, Lu MC, Chen JN (2001) Catalytic decomposition of hydrogen peroxide and 2-chlorophenol with iron oxides. *Water Res* 35:2291–2299.
29. Xu J, Bhattacharyya D (2007) Fe/Pd nanoparticle immobilization in microfiltration membrane pores: Synthesis, characterization, and application in the dechlorination of polychlorinated biphenyls. *Ind Eng Chem Res* 46:2348–2359.
30. Winnik FM, et al. (1998) Polyacrylic acid pore-filled microporous membranes and their use in membrane-mediated synthesis of nanocrystalline ferrihydrite. *Can J Chem* 76:10–17.
31. Gabriel EM, Gillberg GE (1993) *In situ* modification of microporous membranes. *J Appl Polym Sci* 48:2081–2090.